Regulation of *CCL2* expression in human vascular endothelial cells by a neighboring divergently transcribed long noncoding RNA

Nadiya Khyzha[a,b,c], Melvin Khor[a,b,c], Peter V. DiStefano[a,b,c], Liangxi Wang[d,e], Ljubica Matic[f], Ulf Hedin[f], Michael D. Wilson[d,e], Lars Maegdefessel[g,h,i], and Jason E. Fish[a,b,c,1]

[a]Toronto General Hospital Research Institute, University Health Network, Toronto, ON M5G 2C4, Canada; [b]Department of Laboratory Medicine & Pathobiology, University of Toronto, Toronto, ON M5S 1A1, Canada; [c]Peter Munk Cardiac Centre, University Health Network, Toronto, ON M5G 2C4, Canada; [d]Genetics and Genome Biology, SickKids Research Institute, Toronto, ON M5G 0A4, Canada; [e]Department of Molecular Genetics, University of Toronto, Toronto, ON M5S 1A1, Canada; [f]Vascular Surgery, Department of Molecular Medicine and Surgery, Karolinska Institute, 17176 Stockholm, Sweden; [g]Department of Vascular and Endovascular Surgery, Technical University Munich, 81675 Munich, Germany; [h]Partner Site Munich, Deutsches Zentrum für Herz-Kreislauf-Forschung, 80636 Munich, Germany; and [i]Department of Medicine, Karolinska Institute, 17164 Stockholm, Sweden

Edited by Christopher K. Glass, University of California San Diego, La Jolla, CA, and approved June 26, 2019 (received for review March 8, 2019)

Atherosclerosis is a chronic inflammatory disease that is driven, in part, by activation of vascular endothelial cells (ECs). In response to inflammatory stimuli, the nuclear factor kappa-light-chain-enhancer of activated B cells (NF-κB) signaling pathway orchestrates the expression of a network of EC genes that contribute to monocyte recruitment and diapedesis across the endothelium. Although many long noncoding RNAs (lncRNAs) are dysregulated in atherosclerosis, they remain poorly characterized, especially in the context of human vascular inflammation. Prior studies have illustrated that lncRNAs can regulate their neighboring protein-coding genes via interaction with protein complexes. We therefore identified and characterized neighboring interleukin-1β (IL-1β)–regulated messenger RNA (mRNA)–lncRNA pairs in ECs. We found these pairs to be highly correlated in expression, especially when located within the same chromatin territory. Additionally, these pairs were predominantly divergently transcribed and shared common gene regulatory elements, characterized by active histone marks and NF-κB binding. Further analysis was performed on *lncRNA-CCL2*, which is transcribed divergently to the gene, *CCL2*, encoding a proatherosclerotic chemokine. *LncRNA-CCL2* and *CCL2* showed coordinate up-regulation in response to inflammatory stimuli, and their expression was correlated in unstable symptomatic human atherosclerotic plaques. Knock-down experiments revealed that *lncRNA-CCL2* positively regulated *CCL2* mRNA levels in multiple primary ECs and EC cell lines. This regulation appeared to involve the interaction of *lncRNA-CCL2* with RNA binding proteins, including HNRNPU and IGF2BP2. Hence, our approach has uncovered a network of neighboring mRNA–lncRNA pairs in the setting of inflammation and identified the function of an lncRNA, *lncRNA-CCL2*, which may contribute to atherogenesis in humans.

long noncoding RNA | chromatin | atherosclerosis | endothelium | epigenetics

Atherosclerosis is a chronic inflammatory vascular disease characterized by fatty plaque build-up within the arterial wall, and culminates in the development of coronary artery disease. Vascular inflammation plays a pivotal role in the initiation and progression of atherosclerosis (1). In response to inflammatory stimuli, vascular endothelial cells (ECs) become activated via the nuclear factor kappa-light-chain-enhancer of activated B cells (NF-κB) signaling pathway. This NF-κB–dependent transcriptional program leads to the increased production of a network of proinflammatory cytokines, chemokines, and adhesion molecules that facilitate monocyte recruitment and adhesion (1). Following extravasation into the vessel wall, monocytes differentiate into macrophages, which contribute to the growth and subsequent destabilization of plaques. Understanding the molecular mechanisms that control vascular inflammation is imperative for developing new methodologies to limit the progression of atherosclerosis.

Accumulating evidence has shown that long noncoding RNAs (lncRNAs) are dysregulated in atherosclerosis (2, 3); however, only a handful of studies have assessed their functional involvement in regulating inflammatory pathways (4–12), and relatively little is known about their contribution to human vascular EC inflammation. LncRNAs are defined as a heterogeneous class of noncoding transcripts >200 base pairs in length (13, 14). They can be found within the nucleus or the cytoplasm or in both cellular compartments (14). A proportion of lncRNAs have been reported to act in *cis*, meaning that they act near their site of transcription to regulate the expression of neighboring messenger RNA (mRNA) transcripts (15–19), while others have been shown to act in *trans* in areas far from their site of transcription (20, 21). The mechanisms of action of lncRNAs are varied and

Significance

Controlling vascular inflammation is critical for limiting the progression of chronic vascular diseases such as atherosclerosis. Although poorly studied in the context of human vascular inflammation, long noncoding RNAs (lncRNAs) have the potential to regulate their neighboring genes. However, what constitutes a neighboring lncRNA is currently not well defined. In this study, we took an innovative approach to define IL-1β–regulated neighboring mRNA–lncRNA pairs based on colocalization within the same chromatin neighborhood and divergent transcriptional orientation. This approach led to the discovery of *lncRNA-CCL2*, which positively regulates its neighboring gene, *CCL2*, an important player in atherogenesis. Furthermore, *lncRNA-CCL2* is relevant to human disease, as it is elevated in human atherosclerotic plaques, and, given its regulatory role, it may contribute to atherogenesis.

Author contributions: N.K. and J.E.F. designed research; N.K., M.K., P.V.D., and L. Matic performed research; N.K., M.K., P.V.D., L.W., L. Matic, U.H., M.D.W., L. Maegdefessel, and J.E.F. analyzed data; and N.K. and J.E.F. wrote the paper.

The authors declare no conflict of interest.

This article is a PNAS Direct Submission.

Data deposition: Microarray data generated in this study have been deposited in the Gene Expression Omnibus (GEO) database, https://www.ncbi.nlm.nih.gov/geo (accession no. GSE127990). Code used in the analysis can be accessed at https://github.com/nadiyakhyzha/lncRNA_mRNA_neighboring_analysis. A higher-quality Fig. 7 is available at Figshare (DOI: 10.6084/m9.figshare.8956868.v1).

[1]To whom correspondence may be addressed. Email: jason.fish@utoronto.ca.

This article contains supporting information online at www.pnas.org/lookup/suppl/doi:10.1073/pnas.1904108116/-/DCSupplemental.

Published online July 26, 2019.

stem from their ability to interact with RNA, DNA, and proteins (13, 14). For example, lncRNAs can act as guides or decoys to either help recruit or repel a wide range of proteins, including chromatin remodeling complexes, transcription factors, and RNA-binding proteins (12, 22–25). The functionality of the lncRNA, however, is not limited to the transcript itself, as others have shown that lncRNA transcription can be functionally important, as is the case with *Airn* and *Blustr* (16, 26); meanwhile, others have found lncRNA-associated regulatory DNA elements to be important, as is the case with *Haunt*, *Lockd*, and *Pantr1* (27–29).

Given the potential for lncRNAs to regulate their neighboring genes, we aimed to discover *cis*-regulatory lncRNAs involved in vascular inflammation. Features defining *cis*-regulatory lncRNAs, such as the genomic distance between the lncRNA and its regulated mRNA, however, are not well established in the literature (15, 30, 31). Therefore, we set out to systematically define what constitutes a neighboring mRNA–lncRNA pair. We identified neighboring mRNA–lncRNA pairs differentially expressed in ECs stimulated with the proinflammatory cytokine, interleukin-1β (IL-1β). A strong positive correlation in IL-1β responsiveness of the mRNA–lncRNA pairs was observed, but it significantly weakened once the pairs were farther than 100 kilobase pairs (kbp) away from each other. Interestingly, chromatin organization played a more important role than physical distance along the chromosome, as mRNA–lncRNA pairs localized within the same topologically associated domain (TAD) showed the highest correlation, irrespective of the distance between them (32). Additionally, we noted that IL-1β–responsive mRNA–lncRNA pairs were predominantly transcribed in a divergent orientation to each other, and shared regulatory elements, including NF-κB–bound enhancers and promoters. Follow-up functional experiments were performed on *lncRNA-CCL2*, an lncRNA transcribed divergently to the proatherosclerotic chemokine gene, *CCL2*, which encodes monocyte chemoattractant protein 1 (MCP1) (33). Due to its role in monocyte recruitment, MCP1 has been implicated in multiple human diseases, including atherosclerosis (33). We validated *lncRNA-CCL2* to be a *cis*-regulatory lncRNA, as it positively regulated *CCL2* levels. Pull-down experiments suggested that *lncRNA-CCL2* may regulate *CCL2* levels via interaction with RNA-binding proteins. In particular, insulin growth factor 2 binding protein (IGF2BP2) and HNRNPU bound to *lncRNA-CCL2*, and modulation of their abundance affected *CCL2* levels during IL-1β stimulation. Apart from being up-regulated during acute inflammation in vitro, *lncRNA-CCL2* was found to be elevated and correlated with *CCL2* expression in unstable symptomatic human atherosclerotic plaques, which suggests its potential regulatory role during disease development. Overall, our work has taken a unique approach to identify IL-1β–regulated neighboring mRNA–lncRNA pairs and has led to the discovery of a functional lncRNA that is dysregulated in human disease.

Results

Identification of IL-1β–Regulated mRNA–lncRNA Neighboring Pairs. To catalog expression changes in neighboring mRNA–lncRNA pairs during the EC response to inflammatory stimuli, human umbilical vein ECs (HUVECs) were treated with the proinflammatory cytokine, IL-1β, for either 4 or 24 h. RNA was isolated and converted to complementary DNA (cDNA), which was then hybridized to the Arraystar Human lncRNA Expression Microarray V3.0 (containing unique probes for 23,089 mRNAs and 21,339 lncRNAs; Dataset S1) (Gene Expression Omnibus [GEO] ID code GSE127990). In total, 630 lncRNAs and 776 mRNAs were differentially expressed (>2-fold change, $P < 0.05$) upon 4-h IL-1β treatment (Fig. 1 *A* and *B* and Dataset S2). Meanwhile, 583 lncRNAs and 873 mRNAs were differentially expressed (>2-fold change, $P < 0.05$) upon 24-h IL-1β treatment (Fig. 1*A* and Dataset S2). For simplicity, we chose to focus our subsequent analyses on the earlier 4-h IL-1β treatment time point, as changes at this time point are more likely to be primary responses to IL-1β treatment. To identify all IL-1β–regulated neighboring mRNA–lncRNA pairs, any lncRNA whose gene body was located up to 500 kbp from the transcriptional start site (TSS) of a differentially expressed (de) mRNA ($mRNA^{de}$) after 4 h of IL-1β treatment was selected, yielding a total of 8,502 $mRNA^{de}$–lncRNA pairs (Fig. 1*B*). Neighboring $mRNA^{de}$–lncRNA pairs were then segregated depending on whether the lncRNA was IL-1β–regulated ($lncRNA^{de}$) or whether there was no change (nc) in lncRNA expression ($lncRNA^{nc}$), resulting in 8,094 $mRNA^{de}$–$lncRNA^{nc}$ pairs and 408 $mRNA^{de}$–$lncRNA^{de}$ pairs. For comparison, an identical pipeline was used to catalog neighboring IL-1β–regulated mRNA–mRNA pairs ($mRNA^{de}$–$mRNA^{nc}$ or $mRNA^{de}$–$mRNA^{de}$) (*SI Appendix*, Fig. S1*A*). This revealed that $mRNA^{de}$–$mRNA^{nc}$ pairs were more common (11,763 pairs) than $mRNA^{de}$–$mRNA^{de}$ pairs (450 pairs). Next, the distribution of genomic distances from the $mRNA^{de}$ to its neighboring transcript(s) was tabulated (*SI Appendix*, Fig. S1*B*). The $mRNA^{de}$ were found to be physically closer to neighboring $lncRNA^{de}$ than $lncRNA^{nc}$ (median 142.6 kbp vs. 205.3 kbp, $P = 3.11 \times 10^{-8}$). A similar observation was made with $mRNA^{de}$ vs. $mRNA^{nc}$ (median 176.0 kbp vs. 217.9 kbp, $P = 1.09 \times 10^{-3}$). Subsequent analyses used genomic distances representative of the first quartile (50 kbp), median (150 kbp), and third quartile (300 kbp) of $mRNA^{de}$–$lncRNA^{de}$ distances (Dataset S3). Across these genomic distances, there were more $mRNA^{de}$ that had a neighboring $lncRNA^{nc}$ than a neighboring $lncRNA^{de}$ (426 vs. 82, 568 vs. 107, and 732 vs. 200, respectively) (*SI Appendix*, Fig. S1*C* and Dataset S3). Additionally, there were fewer $lncRNA^{de}$ neighbors than $lncRNA^{nc}$ neighbors (median 1 vs. 2 to 6, $P < 1 \times 10^{-15}$) per individual $mRNA^{de}$ (*SI Appendix*, Fig. S1*D*). Altogether, these results suggest that, although almost all IL-1β–regulated mRNAs have an lncRNA

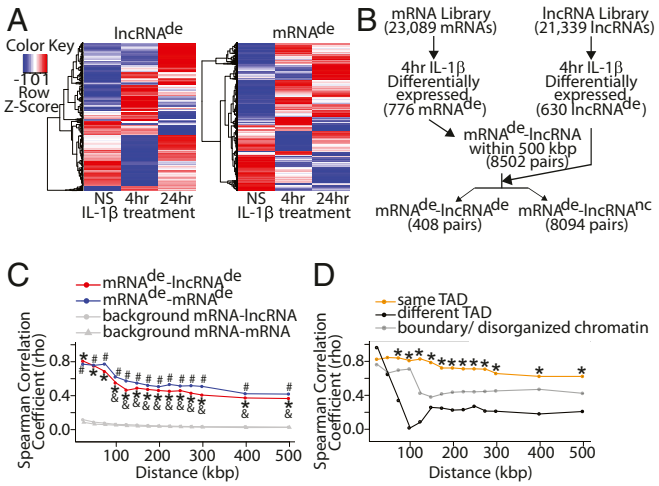

Fig. 1. Identification of IL-1β–regulated mRNA–lncRNA neighboring pairs. (*A*) Microarray heat maps of differentially expressed (de) (>2-fold change, $P < 0.05$) lncRNAs and mRNAs upon 4 or 24 h IL-1β treatment. NS, not stimulated. (*B*) Schematic of the computational pipeline used to identify neighboring $mRNA^{de}$–$lncRNA^{de}$ pairs (4 h IL-1β vs. NS); nc, no change. (*C*) Spearman correlation coefficients for $mRNA^{de}$–$lncRNA^{de}$ and $mRNA^{de}$–$mRNA^{de}$ pairs as a function of genomic distance between them. Background correlation was established using all mRNA–lncRNA and all mRNA–mRNA neighboring pairs possible given the genomic distance between them. Decreasing correlation was observed with increasing distance between $mRNA^{de}$–$lncRNA^{de}$ pairs. *$P < 0.05$, Fisher z transformation with Bonferroni correction, $mRNA^{de}$–$lncRNA^{de}$ vs. all mRNA–lncRNA; #$P < 0.05$, Fisher z transformation with Bonferroni correction, $mRNA^{de}$–$mRNA^{de}$ vs. all mRNA–mRNA; &$P < 0.05$, Fisher z transformation with Bonferroni correction, $mRNA^{de}$–$lncRNA^{de}$ at specified distance vs. $mRNA^{de}$–$lncRNA^{de}$ 25 kbp. (*D*) Spearman correlation coefficients of transcript pairs found either on the same TAD, different TAD, or on boundary/disorganized chromatin. *$P < 0.05$, Fisher z transformation with Bonferroni correction, same TAD vs. different TAD at the specified distance.

located within 500 kbp, very few of these lncRNAs are also IL-1β–regulated.

mRNA^{de}–lncRNA^{de} Pairs Demonstrate a Coordinated Response to IL-1β, Especially When Localized on the Same Topologically Associated Domain. Next, we explored features pertaining to the mRNA^{de}–lncRNA^{de} pairs identified in our study. First, we noted that mRNA^{de} and their neighboring lncRNA^{de} had a coordinate response to IL-1β stimulation, meaning that the neighboring transcript pairs were either both up- or down-regulated by IL-1β. Particularly, we observed a moderate to strong positive correlation in expression fold change upon IL-1β stimulation of mRNA^{de}–lncRNA^{de} pairs which weakened with increasing genomic distance between the mRNA^{de}–lncRNA^{de} pair (Spearman $\rho = 0.805$ for 25 kbp vs. Spearman $\rho = 0.549$ for 100 kbp, $P = 0.023$) (Fig. 1*C*, *SI Appendix*, Fig. S2*A*, and Dataset S4). This coordinate response to IL-1β was not unique to mRNA^{de}–lncRNA^{de} pairs, as the correlation was not significantly different from that of mRNA^{de}–mRNA^{de} pairs (Spearman $\rho = 0.488$ vs. 0.548 for 150 kbp, $P = 1.0$). These findings are not unexpected and are consistent with those reported by other groups (14, 34–37). We next assessed the natural background correlation in responsiveness to IL-1β of neighboring genes by measuring the correlation of all mRNA–lncRNA or mRNA–mRNA neighboring pairs possible given the microarray probes available within a given distance of each other (Fig. 1*C*, *SI Appendix*, Fig. S2*B*, and Dataset S4). The correlation observed in mRNA^{de}–lncRNA^{de} and mRNA^{de}–mRNA^{de} pairs was significantly higher than that of the natural background (Spearman $\rho = 0.805$–0.366 for mRNA^{de}-lncRNA^{de} vs. spearman $\rho = 0.086$–0.026 for all mRNA-lncRNA, $P < 1 \times 10^{-8}$). This result is in line with our previous observation that, although most IL-1β–regulated transcripts will have a neighboring transcript, very few of those will also be IL-1β–regulated (*SI Appendix*, Fig. S1 *C* and *D*). Lastly, permutation tests were performed, and no correlation was found between random mRNA^{de}–lncRNA^{de} and random mRNA^{de}–mRNA^{de} pairs that are not neighboring each other (*SI Appendix*, Fig. S2*C*).

It is becoming increasingly apparent that the genome is divided into chromatin neighborhoods, which are composed of TADs, where there is a high degree of chromatin interaction within, but not between, adjacent TADs (38). Gene coregulation is typically observed within a TAD (32, 39), but has not been explored in the setting of mRNA–lncRNA pairs. We found that, when the mRNA^{de}–lncRNA^{de} pair was located on the same TAD, this was associated with stronger correlation in expression of mRNA^{de}–lncRNA^{de} pairs compared with being on different TADs (Spearman $\rho = 0.79$ vs. 0.26 for 150 kbp, $P = 9.56 \times 10^{-5}$) (Fig. 1*D* and Dataset S4) (GEO ID code for endothelial TADs: GSE63525) (40). Strikingly, the correlation of mRNA^{de}–lncRNA^{de} pairs located on the same TAD did not significantly weaken with increasing genomic distance (Spearman $\rho = 0.825$ for 25 kbp vs. Spearman $\rho = 0.656$ for 300 kbp, $P = 1.0$) (Fig. 1*D* and Dataset S4). Hence, genomic distance alone may be an overly simplistic approach for defining neighboring mRNA^{de}–lncRNA^{de} pairs. Instead, our data suggest that localization within the same chromatin neighborhood (i.e., TAD) should be considered when seeking to identify neighboring genes.

Divergent Transcription Is a Common Feature of mRNA^{de}–lncRNA^{de} Pairs. To gain further mechanistic insight into the regulation of mRNA^{de}–lncRNA^{de} pairs, the presence of genomic regulatory elements in their vicinity was explored. Previously published RELA (NF-κB subunit) and H3K27ac (histone mark characteristic of active enhancers and promoters) chromatin immunoprecipitation sequence (ChIP-seq) data (GEO ID code GSE89970) from 4-h IL-1β–stimulated human aortic ECs was utilized for analysis (41). Intriguingly, mRNA^{de}–lncRNA^{de} pairs, on average, had stronger intensities of RELA and H3K27ac ChIP-seq signals between the 2 transcripts compared with 50 kbp upstream or downstream of the transcript pair, or compared with background (random sampling within the chromosomes containing neighboring transcript pairs of the same size range as the neighboring transcript pair). This observation held true for mRNA^{de}–lncRNA^{de} pairs 50 and 150 kbp apart and was evident, to a lesser extent, for those 300 kbp apart (*SI Appendix*, Fig. S3 *A*–*C*). In contrast, mRNA^{de}–mRNA^{de} pairs did not follow the same trend, which may suggest differences in how they are organized in the genome relative to mRNA^{de}–lncRNA^{de} pairs (*SI Appendix*, Fig. S3 *A*–*C*).

The presence of regulatory elements between mRNA^{de}–lncRNA^{de} pairs prompted us to examine the transcriptional orientation of mRNA^{de}–lncRNA^{de} pairs with respect to each other and the shared regulatory element(s). Specifically, mRNA^{de}–lncRNA^{de} pairs were characterized as being divergent, antisense, forward codirectional, reverse codirectional, convergent, or intersecting with respect to each other. The proportion of different transcriptional orientation types significantly differed between mRNA^{de}–lncRNA^{de} and mRNA^{de}–mRNA^{de} pairs that were 50, 150, and 300 kbp apart (Fig. 2*A* and Dataset S5). While mRNA^{de}–lncRNA^{de} pairs were most frequently divergent (40.2/36.3/32.2% vs. 17.1/15.3/16.9% of total, 50/150/300 kbp mRNA^{de}–lncRNA^{de} vs. mRNA^{de}–mRNA^{de}, respectively, $P < 0.004$), mRNA^{de}–mRNA^{de} pairs were most commonly forward codirectional (15.2/23.3/24.8% vs. 51.4/48.8/41.3% of total, 50/150/300 kbp mRNA^{de}–lncRNA^{de} vs. mRNA^{de}–mRNA^{de}, respectively, $P < 0.004$). However, we did observe that all possible mRNA–lncRNA pairs in our dataset also enriched for divergent transcription—suggesting inherent organization of mRNA–lncRNA pairs into divergent orientations across the genome (40.2/36.3/32.2% vs. 32.0/28.4/28.3% of total, 50/150/300 kbp mRNA^{de}–lncRNA^{de} vs. all mRNA–lncRNA, respectively, $P > 0.25$) (Fig. 2*A* and Dataset S5). We then assessed whether divergent mRNA^{de}–lncRNA^{de} pairs were more likely to have shared regulatory elements between them compared with nondivergent pairs. Indeed, divergent mRNA^{de}–lncRNA^{de} pairs that were 50, 150, and 300 kbp apart, on average, had stronger intensities of RELA and H3K27ac ChIP-seq signals between them compared with nondivergent mRNA^{de}–lncRNA^{de} pairs (Fig. 2*B* and *SI Appendix*, Fig. S3 *D* and *E*). This observation was especially pronounced for divergent mRNA^{de}–lncRNA^{de} pairs that were on the same TAD (Fig. 2*C*). Furthermore, divergent mRNA^{de}–lncRNA^{de} pairs exhibited stronger correlation in IL-1β–induced expression fold change than mRNA^{de}–lncRNA^{de} pairs transcribed in nondivergent orientations (i.e., Spearman $\rho = 0.68$ vs. $\rho = 0.35$ at 200 kbp, $P = 0.028$; Spearman $\rho = 0.56$ vs. $\rho = 0.29$ at 500 kbp, $P = 0.045$) (Fig. 2*D*, *SI Appendix*, Fig. S4*A*, and Dataset S5). Hence, we interpret these data to indicate that these divergent mRNA^{de}–lncRNA^{de} pairs are coregulated through shared regulatory elements located between their transcriptional units.

Next, the functional significance of divergently transcribed lncRNAs was pursued. Given that *cis*-acting lncRNAs have been reported to regulate their neighboring mRNAs (15, 36), we tested whether the presence of a neighboring lncRNA^{de} influences mRNA^{de} responsiveness to IL-1β. Taken as a whole, having a neighboring lncRNA^{de} had only a modest influence on mRNA^{de} responsiveness to IL-1β (*SI Appendix*, Fig. S4*B*). However, upon subdividing mRNA^{de}–lncRNA^{de} based on transcriptional orientation, we found that up-regulated mRNA^{de} neighboring a divergent lncRNA^{de} trended toward a higher response to IL-1β than those near a nondivergent lncRNA^{de} (median fold change for 150-kbp distance, 6.07 for divergent, 2.97 for nondivergent, $P = 0.19$) (*SI Appendix*, Fig. S4 *C* and *D*). A possible explanation for this phenomenon is that divergent mRNA^{de}–lncRNA^{de} pairs share stronger regulatory elements, as a recent study utilizing massively parallel reporter assays has shown that promoters of divergent lncRNAs tend to be stronger at driving transcription (42). However, it is plausible that the trend in greater responsiveness to IL-1β could also be attributed to the divergent lncRNA positively regulating its neighboring gene, as another group showed that chromatin-tethered lncRNAs can drive the expression of their neighboring mRNAs. Hence, we further assessed divergent mRNA^{de}–lncRNA^{de} pairs to discover functional lncRNAs.

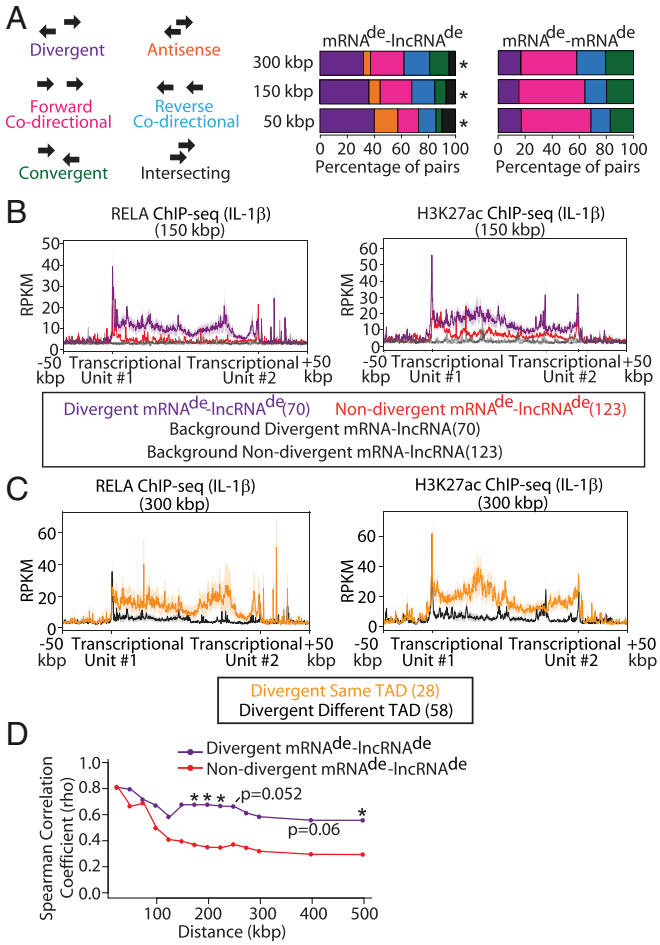

Fig. 2. Divergent transcription is a common feature of mRNA^{de}–lncRNA^{de} pairs. (*A*) Percentage distribution of orientations of mRNA^{de}–lncRNA^{de} vs. mRNA^{de}–mRNA^{de} transcript pairs that are <50, <150, and <300 kbp apart. *P < 0.05, χ^2 test with Bonferroni correction, mRNA^{de}–lncRNA^{de} vs. mRNA^{de}–mRNA^{de}. (*B*) Profile plot of RELA and H3K27ac ChIP-seq signals in IL-1β–treated ECs that fall within the region between divergent and nondivergent mRNA^{de}–lncRNA^{de} that are <150 kbp apart. Background signal was determined based on a random sampling of the same-size regions within the chromosomes containing the neighboring transcript pairs. (*C*) Profile plot of RELA and H3K27ac ChIP-seq signals with IL-1β treatment for regions between divergently transcribed mRNA^{de}–lncRNA^{de} pairs that are on either the same or a different TAD within a 300-kbp window. The number of pairs is indicated in brackets. (*D*) Spearman correlation coefficients for divergent and nondivergent mRNA^{de}–lncRNA^{de} and mRNA^{de}–mRNA^{de} pairs that are of increasing genomic distances apart. *P < 0.05, Fisher z transformation with Bonferroni correction, divergent vs. nondivergent at the specified distance.

Identification and Characterization of Divergent mRNA^{de}–lncRNA^{de} Pairs. To further investigate the regulation of mRNA^{de}–lncRNA^{de} pairs, we identified all divergent pairs that were localized on the same TAD. In total, there were 18 such divergent mRNA^{de}–lncRNA^{de} pairs after removing splice variants, which correspond to 18 unique mRNAs and 15 unique lncRNAs (Fig. 3*A* and Dataset S6). These divergent mRNA^{de}–lncRNA^{de} pairs had a coordinated response to IL-1β demonstrated by strong correlation (Spearman $\rho = 0.896$, $P = 1.49 \times 10^{-9}$) in IL-1β–induced fold change (Fig. 3 *A* and *B*). As expected, the mRNA^{de} from the list were enriched for inflammation-related gene ontology biological processes such as "response to wounding," "inflammatory response," "defense response," and "regulation of cell proliferation" (*SI Appendix*, Fig. S5*A*). The responsiveness of mRNA^{de}–lncRNA^{de} pairs to 4-h IL-1β treatment was successfully validated by qRT-PCR for 10/15 (69%) lncRNAs and 17/18 (94.4%) mRNAs (Fig. 3*A*). Examples of genomic loci of a few successfully validated mRNA^{de}–lncRNA^{de} pairs are shown, namely those of *lncRNA-F3*, *lncRNA-BARD1*, and *lncRNA-CCL2* (Fig. 3*C* and *SI Appendix*, Fig. S5*B*). Importantly, RELA (NF-κB) and H3K27ac ChIP-seq signals were found to be enriched between the mRNA^{de} and lncRNA^{de} transcriptional units.

***CCL2* and *lncRNA-CCL2* Are Coordinately Regulated during Acute Inflammation.** For follow-up experiments, we chose to assess the function of *lncRNA-CCL2* (a previously uncharacterized lncRNA annotated as *TCONS_00025610*), due to the functional relevance of *CCL2*/MCP1 to inflammatory diseases, including atherosclerosis (43). The *lncRNA-CCL2* is a 2-exon transcript spanning ∼33 kbp of DNA (Fig. 3*C* and *SI Appendix*, Table S2). We confirmed its existence by amplification of the full-length spliced transcript from HUVEC cDNA (*SI Appendix*, Table S2). Not only does *lncRNA-CCL2* neighbor *CCL2*, but a number of other *CCL* genes are located in the genomic vicinity, including *CCL7*, *CCL11*, *CCL13*, *CCL8*, and *CCL1* (Fig. 3*C*). The *lncRNA-CCL2* is transcribed through a superenhancer (44) that spans ∼20 kbp and contains multiple RELA (NF-κB subunit) binding peaks (Fig. 3*C*). In primary HUVEC, the transcription of *lncRNA-CCL2* and *CCL2* (as assessed by measuring the unspliced primary transcripts, *pre-lncRNA-CCL2* and *pre-CCL2*) is induced around the same time (i.e., 45 min after IL-1β treatment) (Fig. 4*A*). However, there is a delay in the processing of *lncRNA-CCL2*, as the spliced transcript does not increase in expression until 2 h of IL-1β treatment (Fig. 4*B*). This is consistent with the large intron in *lncRNA-CCL2* that must be spliced out to generate the mature transcript (*SI Appendix*, Table S2). The expression of *lncRNA-CCL2* and *CCL2* is also sustained during long-term treatment with IL-1β, something atypical of other IL-1β–responsive genes, such as *SELE* (Fig. 4*C*). Moreover, the expression of *lncRNA-CCL2* and *CCL2* is maintained after removal of IL-1β, and they do not exhibit desensitization to IL-1β exposure, which is in contrast to *SELE* (*SI Appendix*, Fig. S6). The induction of *lncRNA-CCL2* and

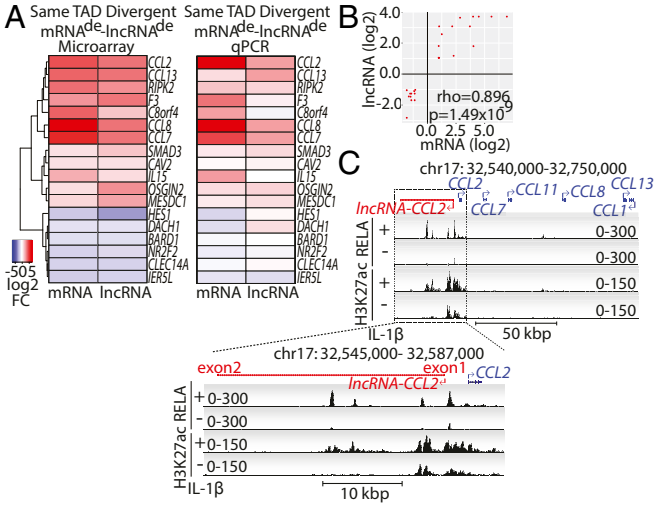

Fig. 3. Identification and characterization of divergent mRNA^{de}–lncRNA^{de} pairs. (*A*) Divergent mRNA^{de}–lncRNA^{de} pairs found within the same TAD are displayed. Heatmap showing the log2 fold-change (FC) in response to 4 h of IL-1β treatment based on microarray (*Left*) and qPCR validation (*Right*) are shown. (*B*) Scatterplot showing the log2 FCs of mRNA^{de} on the *y* axis and the log2 FCs of their neighboring divergent lncRNA^{de} on the *x* axis. Spearman rho correlation coefficient and its associated *P* value are indicated. (*C*) University of California, Santa Cruz genome browser tracks depicting *lncRNA-CCL2*. ChIP-seq tracks are shown for RELA and H3K27ac under either basal conditions or upon IL-1β treatment. Zoom-in of *lncRNA-CCL2* shows that it is a 2-exon transcript spanning 32.8 kbp of DNA.

CCL2 in response to IL-1β was also evident in EC lines, namely human microvascular ECs (HMEC1) and immortalized umbilical vein ECs (EC-RF24) (Fig. 4*D*). However, the absolute copy number of *lncRNA-CCL2* and *CCL2* differed between EC types. In particular, the EC-RF24 and HMEC1 cell lines had lower copy numbers of *CCL2* and *lncRNA-CCL2* than HUVEC. Across all cell lines, *CCL2* transcript copy number was ∼5,300-fold higher than that of *lncRNA-CCL2* (*CCL2*, $\sim 3.2 \times 10^8$ vs. 5.3×10^9 copies per 1 μg of RNA; *lncRNA-CCL2*, $\sim 1.8 \times 10^5$ vs. 1×10^6 copies per 1 μg of RNA; EC-RF24/HMEC1 vs. HUVEC). Aside from IL-1β stimulation, *lncRNA-CCL2* and *CCL2* were also coordinately induced by other proinflammatory stimuli such as lipopolysaccharide (LPS) and tumor necrosis factor alpha (TNF-α) (Fig. 4*E*). Neither transcript was inducible by vascular endothelial cell growth factor (VEGF) or transforming growth factor beta (TGF-β) stimulation. Lastly, inhibitor experiments demonstrated that *lncRNA-CCL2* and *CCL2* were regulated by NF-κB, p300, and BRD4, as seen using inhibitors of IκB kinase 2 (i.e., TPCA-1), p300/CBP (i.e., C646), and BRD4 (i.e., JQ1) (Fig. 4*F*). Thus, in ECs, *lncRNA-CCL2* and *CCL2* are a divergently transcribed transcript pair that shows synchronized responses to proinflammatory stimuli. Interestingly, a number of other IL-1β–regulated chemokine genes are clustered near the *CCL2* superenhancer, including *CCL7*, *CCL11*, *CCL8*, *CCL13*, and *CCL1* (Fig. 3*C*). While *lncRNA-CCL2*, *CCL2*, and *CCL7* followed similar kinetics, the other *CCL* genes in this locus responded to IL-1β with differing kinetics, suggesting potential differences in their regulation (*SI Appendix*, Fig. S7).

***LncRNA-CCL2* Positively Regulates Levels of Its Neighboring *CCL2* Gene.** The functional role of *lncRNA-CCL2* was explored using 2 different knockdown approaches. Small interfering RNA (siRNA) and antisense locked nucleic acid (LNA) GapmeR were designed to target exon 2 of *lncRNA-CCL2*. Exon 2 was targeted as it is 15 kbp distal to the superenhancer, and therefore siRNAs and GapmeRs targeting this region should not directly interfere with the activity of the superenhancer (Fig. 3*C*). We were able to achieve sufficient knockdown of the spliced *lncRNA-CCL2* transcript (Fig. 5 *A* and *B*), but not the *pre-lncRNA-CCL2* transcript (*SI Appendix*, Fig. S8*A*). Knockdown of *lncRNA-CCL2* using either siRNA or GapmeR led to a ∼50% decrease in *CCL2* expression upon IL-1β stimulation of HUVEC (Fig. 5 *A* and *B*). Levels of the unspliced *pre-CCL2* were likewise decreased upon *lncRNA-CCL2* knockdown (Fig. 5*C* and *SI Appendix*, Fig. S8*B*). Furthermore, we were able to recapitulate the effect of *lncRNA-CCL2* knockdown on *CCL2* levels in the EC lines, EC-RF24 and HMEC1 (Fig. 5 *D* and *E*). A strong positive correlation between the degree of *lncRNA-CCL2* knockdown and the decrease in *CCL2* induction was observed ($r = 0.8040$, $P = 0.0634$) (*SI Appendix*, Fig. S8*C*). However, we did not find significant changes in basal *CCL2* levels, which may be due to the

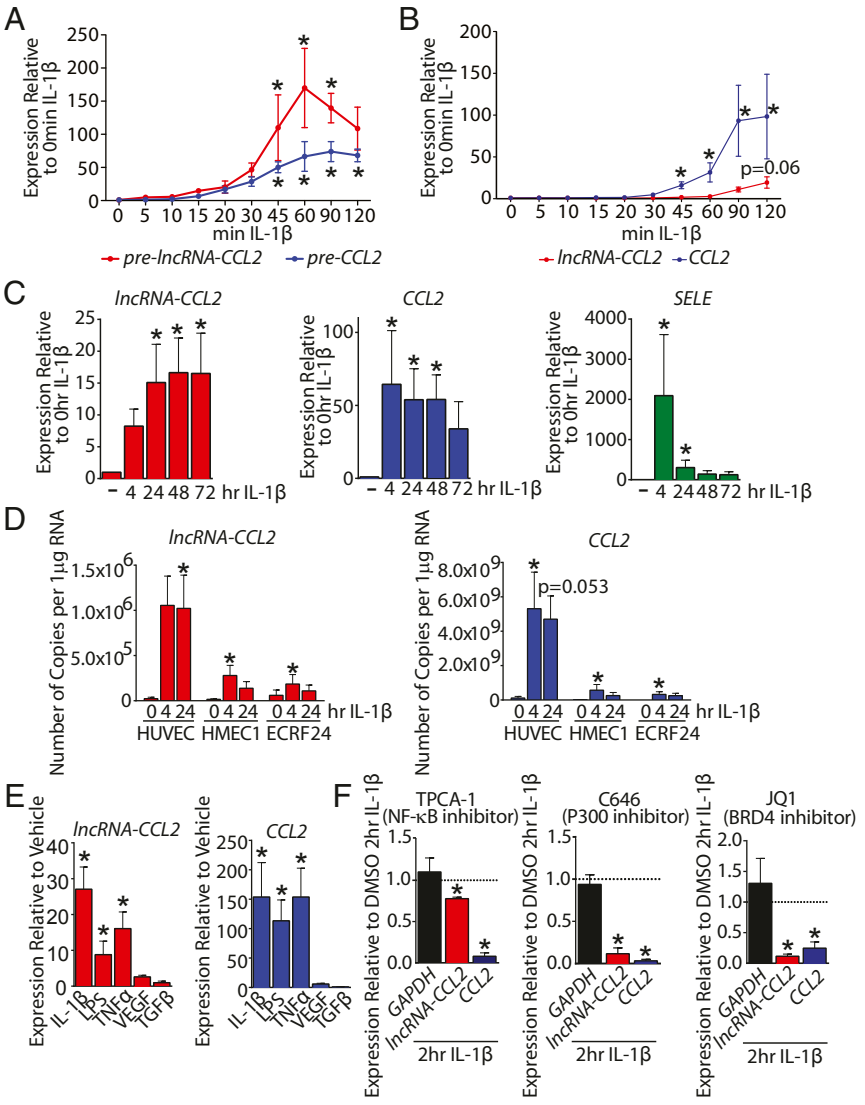

Fig. 4. *CCL2* and *lncRNA-CCL2* are coordinately regulated during acute inflammation. (*A*) The qRT-PCR data of unspliced *pre-lncRNA-CCL2* and *pre-CCL2* upon treatment with IL-1β for various lengths of time. *$P < 0.05$, Friedman test with Dunn's multiple comparisons test, relative to basal, $n = 3$ to 4. (*B*) The qRT-PCR data of spliced *lncRNA-CCL2* and *CCL2* upon treatment with IL-1β for various lengths of time. *$P < 0.05$, Friedman test with Dunn's multiple comparisons test, relative to basal, $n = 5$. (*C*) The qRT-PCR data showing the kinetic response of *lncRNA-CCL2*, *CCL2*, and *SELE* to 4 to 72 h of IL-1β in HUVEC. *$P < 0.05$, Friedman test with Dunn's multiple comparisons test, relative to basal, $n = 6$. (*D*) Copy number of *lncRNA-CCL2* and *CCL2* transcripts per 1 μg of RNA measured using qRT-PCR in HUVEC, HMEC1, and EC-RF24 at multiple time points of IL-1β stimulation. *$P < 0.05$, Friedman test with Dunn's multiple comparisons test, relative to basal, $n = 4$ to 7. (*E*) The qRT-PCR data showing the responsiveness of *lncRNA-CCL2* and *CCL2* to 2 h of IL-1β, LPS, TNFα, VEGF, and TGF-β stimulation in HUVEC. *$P < 0.05$, Friedman test with Dunn's multiple comparisons test, $n = 3$ to 7. (*F*) The qRT-PCR data of *GAPDH*, *lncRNA-CCL2*, and *CCL2* expression upon 1-h pretreatment with chemical inhibitors of NF-κB signaling (TPCA-1), p300 activity (C646), and BRD4 (JQ1) followed by 2 h of IL-1β stimulation in HUVEC. All data are relative to expression values upon DMSO pretreatment followed by 2 h of IL-1β stimulation. *$P < 0.05$, paired Student's *t* test, $n = 3$.

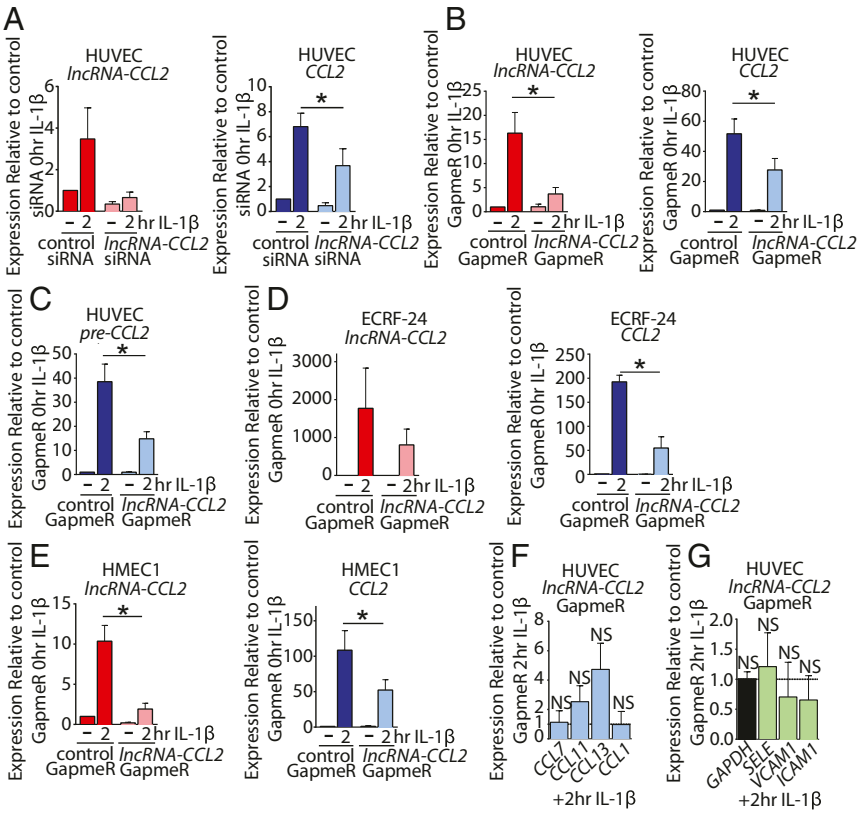

Fig. 5. The *lncRNA-CCL2* positively regulates levels of its neighboring *CCL2* gene. (*A* and *B*) The qRT-PCR data of *lncRNA-CCL2* and *CCL2* gene expression upon knockdown of *lncRNA-CCL2* using (*A*) siRNA or (*B*) GapmeR under basal condition and upon stimulation with IL-1β for 2 h in HUVEC. *$P < 0.05$, paired Student's *t* test, (*A*) $n = 3$, (*B*) $n = 8$. (*C*) The qRT-PCR data of unspliced *pre-CCL2* gene expression upon knockdown of *lncRNA-CCL2* using GapmeR under basal condition and upon stimulation with IL-1β for 2 h in HUVEC. *$P < 0.05$, paired Student's *t* test, $n = 5$. (*D* and *E*) qRT-PCR data of *lncRNA-CCL2* and *CCL2* expression upon knockdown of *lncRNA-CCL2* using GapmeR under basal conditions or upon stimulation with IL-1β for 2 h in (*D*) EC-RF24 and (*E*) HMEC1. *$P < 0.05$, paired Student's *t* test, (*D*) $n = 3$, (*E*) $n = 5$. (*F*) The qRT-PCR data of *CCL* genes upon knockdown of *lncRNA-CCL2* using GapmeR and stimulation with IL-1β for 2 h in HUVEC. *$P < 0.05$, paired Student's *t* test, $n = 4$; NS, nonsignificant. (*G*) The qRT-PCR data of inflammatory genes upon knockdown of *lncRNA-CCL2* using GapmeR and stimulation with IL-1β for 2 h in HUVEC. *$P < 0.05$, paired Student's *t* test, $n = 4$.

low basal levels of *lncRNA-CCL2* (Fig. 5 *A*–*E*). Next, we assessed whether *lncRNA-CCL2* can regulate any of the other genes in the *CCL* gene cluster. No significant changes were observed in the expression of other *CCL* genes upon IL-1β stimulation (Fig. 5*F*), suggesting that *lncRNA-CCL2* only regulates the most proximal *CCL* gene of the cluster, namely *CCL2*. Additionally, no consistent change in expression of the NF-κB responsive genes *SELE*, *ICAM1*, and *VCAM1* was observed (Fig. 5*G* and *SI Appendix*, Fig. S8*D*). This finding suggests that *lncRNA-CCL2* is unlikely to be involved in directly regulating NF-κB signaling. Furthermore, ectopic overexpression of spliced *lncRNA-CCL2* in HUVEC had no effect on *CCL2* expression (*SI Appendix*, Fig. S9). This finding is in line with previous studies in which ectopic expression of *cis*-acting lncRNAs had no effect on their target mRNA, potentially due to the inability of the ectopically expressed lncRNA to properly localize to its target locus (18, 45).

***LncRNA-CCL2* Regulation of *CCL2* Levels May, in Part, Be Mediated through Interaction with RNA-Binding Proteins.** We next sought to explore the mechanism(s) through which *lncRNA-CCL2* regulates *CCL2* levels. Determining the subcellular localization of an lncRNA can give insight into its potential mechanism of action. *LncRNA-CCL2* was detectable in both the nuclear and cytoplasmic compartments, with a modest enrichment in the cytoplasm (Fig. 6*A*). Given the presence of *lncRNA-CCL2* in the cytoplasm, we first verified that it does not encode any proteins. The coding potential of *lncRNA-CCL2* is very low (0.002, according to the Coding-Potential Assessment Tool, with a coding probability of <0.364 indicating a noncoding sequence; *SI Appendix*, Fig. S10*A*) (46). Although it has a potential open reading frame of 29 amino acids, overexpression of *lncRNA-CCL2* did not produce any observable peptides (*SI Appendix*, Fig. S10*B*). Moreover, cytoplasmic lncRNAs typically act in *trans* (31), but we found no evidence of *lncRNA-CCL2* globally regulating inflammatory genes (i.e., *SELE*, *VCAM1*, and *ICAM1*). Thus, it is unlikely that *lncRNA-CCL2* acts in *trans* to indirectly regulate *CCL2* via modulating NF-κB signaling. For this reason, we next queried whether the nuclear fraction of *lncRNA-CCL2* is responsible for regulating *CCL2* in *cis*.

Cis-acting lncRNAs have previously been shown to interact with transcription factors and chromatin remodeling complexes (15). Hence, we probed for the interaction of *lncRNA-CCL2* with *CCL2* superenhancer-associated chromatin machinery (44). However, we found no reproducible binding of *lncRNA-CCL2* to RELA, p300, or BRD4 (*SI Appendix*, Fig. S11*A*). An unbiased approach was next used to identify nuclear interacting protein partners of *lncRNA-CCL2* by performing an RNA pull-down experiment. To accomplish this, a biotinylated *lncRNA-CCL2* probe or a *scramble* probe (*SI Appendix*, Table S2) was incubated with nuclear lysates of IL-1β–stimulated HMECs. Mass spectrometry of the isolated proteins revealed 49 proteins that uniquely bound and 9 proteins that enriched for binding to the *lncRNA-CCL2* probe (Dataset S7). Interaction of CHD4 with *lncRNA-CCL2* was confirmed by CHD4 immunoprecipitation (*SI Appendix*, Fig. S11*B*). However, *CHD4* knockdown experiments revealed that CHD4 played no role in modulating *CCL2* levels during inflammation (*SI Appendix*, Fig. S11*C*).

Functional annotation of the proteins pulled down with *lncRNA-CCL2* revealed that they were predominantly enriched for RNA-binding proteins such as members of the IGF2BP and the heterogeneous ribonucleoprotein (HNRNP) families (Fig. 6*B*). This finding was intriguing, as we found differences in the transcript stability of *lncRNA-CCL2* and *CCL2* (*SI Appendix*, Fig. S12), implying that RNA-binding proteins may participate in their regulation. In particular, we noted *lncRNA-CCL2* to have a longer half-life than *CCL2* in actinomycin D experiments (>240 min for *lncRNA-CCL2* vs. <60 min for *CCL2*). Hence, we focused on RNA-binding proteins, IGF2BP2, IGF2BP3, and HNRNPU, as they have previously been shown to interact with lncRNAs (47–51) and have been shown to modulate mRNA stability (52–54). We confirmed that HNRNPU and IGF2BP2 bind specifically to an *lncRNA-CCL2* probe, but not to a *scramble* probe (Fig. 6*C*). We then explored whether these proteins could modulate *CCL2* levels by performing siRNA-mediated knock

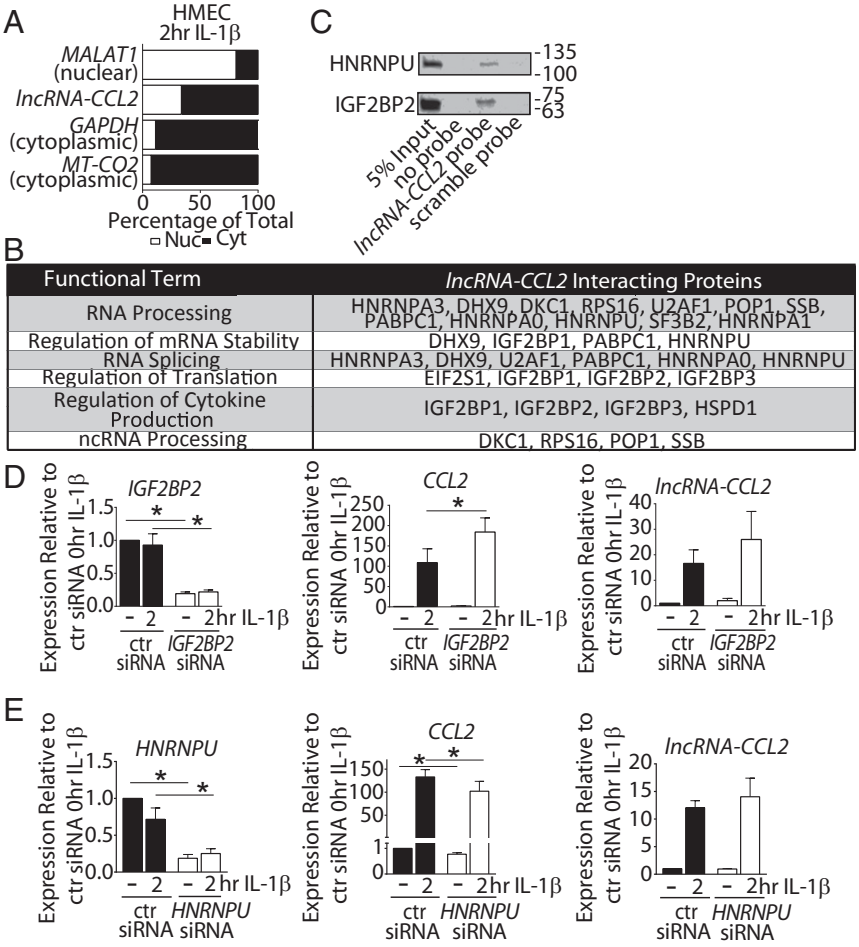

Fig. 6. The regulation of *CCL2* levels by *lncRNA-CCL2* may, in part, be mediated through interaction with RNA-binding proteins. (*A*) The qRT-PCR data showing the distribution of *MT-CO*$_2$ (cytoplasmic control), *GAPDH* (cytoplasmic control), *lncRNA-CCL2*, and *MALAT1* (nuclear control) in the nuclear and cytoplasmic compartments of 2-h IL-1β–stimulated HMEC1, $n = 3$. (*B*) Table showing the functional terms associated with the proteins uniquely pulled down or enriched in pull-downs using a biotinylated *lncRNA-CCL2* probe in nuclear extracts of IL-1β–stimulated HMEC1. (*C*) Validation of IGF2BP2 and HNRNPU pull-down with the biotinylated *lncRNA-CCL2* probe by Western blot. (*D*) The qRT-PCR data of *IGF2BP2*, *lncRNA-CCL2*, and *CCL2* expression upon knockdown of *IGF2BP2* using siRNA under basal and 2-h IL-1β–stimulated conditions in HMEC1. $*P < 0.05$, paired Student's *t* test, $n = 4$. (*E*) The qRT-PCR data of *HNRNPU*, *lncRNA-CCL2*, and *CCL2* expression upon knockdown of *HNRNPU* using siRNA under basal and 2-h IL-1β–stimulated conditions in HMEC1. $*P < 0.05$, paired Student's *t* test, $n = 4$.

down of *IGF2BP2*, *IGF2BP3*, and *HNRNPU* in HMECs. Varying effects on *CCL2* levels were observed with each of these 3 proteins. In the case of *IGF2BP3*, its knockdown resulted in no change in *CCL2* or *lncRNA-CCL2* levels during IL-1β stimulation (*SI Appendix*, Fig. S13). Meanwhile, knockdown of *IGF2BP2* significantly increased the level of *CCL2*, while there was no significant change in *lncRNA-CCL2* during IL-1β stimulation (Fig. 6*D*). Lastly, knockdown of *HNRNPU* resulted in a significant decrease in *CCL2* but not *lncRNA-CCL2* during IL-1β stimulation (Fig. 6*E*). These results imply that IGF2BP2 and HNRNPU may, in part, contribute to the regulation of *CCL2* by *lncRNA-CCL2*. Taken together, these findings suggest that *lncRNA-CCL2* may act as a scaffold for RNA-binding proteins that both positively and negatively regulate *CCL2* levels.

***LncRNA-CCL2* Is Elevated in Unstable Symptomatic Human Atherosclerotic Plaques Where It Correlates with *CCL2* Expression.** While we have provided evidence that *lncRNA-CCL2* is regulated in vitro by inflammatory stimuli, we sought to determine whether the expression of *lncRNA-CCL2* is relevant to chronic inflammatory pathologies such as atherosclerosis. To do so, levels of *lncRNA-CCL2* and *CCL2* were assessed in human atherosclerotic plaques isolated from patients undergoing carotid endarterectomy (CEA, $n = 127$) and belonging to the Biobank of Karolinska Endarterctomies (BiKE), Karolinska Institute. Patients were characterized as either stable asymptomatic ($n = 40$) or unstable symptomatic ($n = 87$), where "symptomatic" indicates that the patient has experienced a mild embolic event, particularly, either a transient ischemic attack, a minor stroke, or temporary loss of vision (i.e., amaurosis fugax) (55). As a control, healthy arteries ($n = 10$) were used from organ donors with no previous history of cardiovascular disease. Based on the microarray, *lncRNA-CCL2* and *CCL2* were significantly elevated in both unstable symptomatic and stable asymptomatic plaques (Fig. 7*A*). However, the probe capturing *lncRNA-CCL2* (236469_at) was not uniquely specific to *lncRNA-CCL2* and aligned to other mRNAs in the human genome. Thus, to validate the microarray and to more accurately assess *lncRNA-CCL2* expression, real-time qPCR (RT-qPCR) was performed with primers that spanned exon 1 and exon 2 (as used in our in vitro experiments) on a smaller set of CEA and control samples. RT-qPCR revealed that *lncRNA-CCL2* was significantly elevated in unstable symptomatic plaques (Fig. 7*B*). Furthermore, we observed a positive correlation between the expression of *lncRNA-CCL2* and *CCL2* in unstable symptomatic plaque samples ($r = 0.78$, $P = 0.0222$) (Fig. 7*C*). This observation in unstable symptomatic plaques is in line with our previous in vitro findings that *lncRNA-CCL2* and *CCL2* are correlated in expression in response to IL-1β treatment and that *lncRNA-CCL2* positively regulates *CCL2* expression in ECs. However, atherosclerotic plaques comprise more than just ECs, and changes in the cell type composition of plaques could also affect the relative levels of *lncRNA-CCL2* and *CCL2* (56, 57). Next, using RNA in situ hybridization, it was observed that *lncRNA-CCL2* was expressed in the highly inflamed shoulder regions and fibrous caps of stable asymptomatic plaques (Fig. 7*D*). In unstable symptomatic plaques, *lncRNA-CCL2* was particularly highly expressed in the ECs overlying the carotid plaque (Fig. 7*D*, arrowhead). Strikingly, *lncRNA-CCL2* appeared to also be expressed in the lining of neovessels within stable asymptomatic and unstable symptomatic plaques (Fig. 7*D*, arrows). Unlike advanced atherosclerotic plaques, only low levels of diffuse signal corresponding to *lncRNA-CCL2* could be

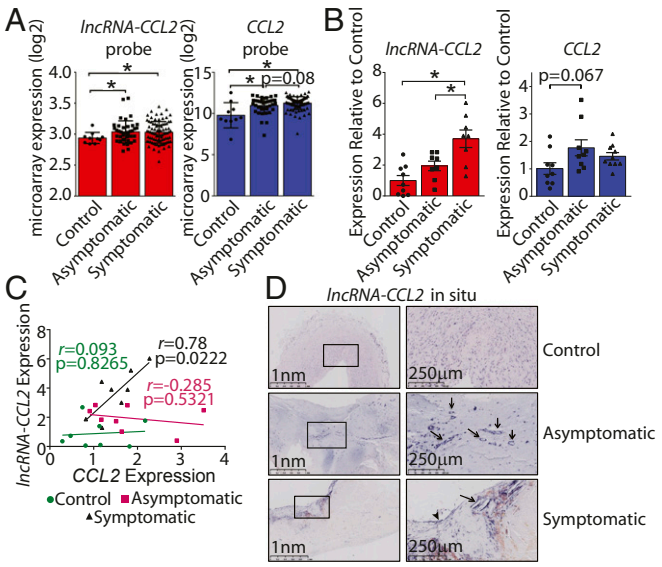

Fig. 7. *LncRNA-CCL2* is elevated in unstable symptomatic human atherosclerotic plaques where it correlates with *CCL2* expression. (*A*) Normalized log2 expression of *lncRNA-CCL2* and *CCL2* probes in microarrays performed on human unstable symptomatic or stable asymptomatic atherosclerotic plaques or healthy artery controls. $*P < 0.05$, ordinary 1-way ANOVA with Sidak correction. (*B*) The qRT-PCR expression of *lncRNA-CCL2* and *CCL2* in human unstable symptomatic or stable asymptomatic atherosclerotic plaques or healthy artery controls. $*P < 0.05$, ordinary 1-way ANOVA with Sidak correction. (*C*) Scatter plot showing the correlation in qRT-PCR expression of *lncRNA-CCL2* and *CCL2* in samples from human unstable symptomatic or stable asymptomatic atherosclerotic plaques or healthy artery controls. The Pearson correlation coefficient (*r*) and its associated *P* values are shown. (*D*) RNA in situ hybridization showing the presence and increased expression of *lncRNA-CCL2* in unstable symptomatic human atherosclerotic plaques compared with healthy artery controls from the BiKE biobank. *LncRNA-CCL2* is expressed in neovessels (arrows) and in the EC lining of the atheroma (arrowhead). Images from 2 different magnifications, 2.5× and 10×, are shown. A higher-quality Fig. 7 is available at Figshare (DOI: 10.6084/m9.figshare.8956868.v1).

detected in undiseased healthy arteries. Altogether, these data suggest that *lncRNA-CCL2* is dysregulated during human atherosclerosis.

Discussion

The discovery that thousands of lncRNAs are encoded in the human genome adds an extra layer to the regulation of gene expression, yet the vast majority of lncRNAs remain uncharacterized. Our study aimed to uncover functional lncRNAs involved in human vascular inflammation with the hopes of finding ways to fine-tune the inflammatory response. A common approach to identifying functional lncRNAs has been to focus on lncRNAs that act in *cis* to regulate their neighboring mRNAs. However, there is currently no systematic way to identify *cis*-acting lncRNAs, as there are no evidence-based guidelines as to what constitutes a "neighboring" mRNA (15, 30). Thus, we sought to precisely define the concept of a neighboring mRNA–lncRNA pair by identifying and characterizing all IL-1β–regulated mRNA–lncRNA pairs separated by varying genome distances. We found that IL-1β–regulated mRNA–lncRNA pairs were correlated in their responsiveness to IL-1β and that this correlation generally decreased with increasing genomic distance. Similar observations have been reported by others who observed coexpression of lncRNAs with their neighboring protein coding genes (14, 58–60), but this had not been previously assessed in the setting of EC activation. Importantly, genomic distance alone does not reflect the actual physical interactions that occur between genomic regions, since the genome is compartmentalized into chromatin neighborhoods that have been referred to as TADs (32, 38, 40). Indeed, our analysis revealed that IL-1β–regulated mRNA–lncRNA pairs on the same TAD were highly correlated regardless of the genomic distance between them. Hence, we argue that defining neighboring transcript pairs based on a genomic distance cutoff alone may be superficial, as it does not take into consideration the genomic neighborhoods in which the transcripts reside.

Currently, "lncRNA" is an umbrella term for a broad class of noncoding transcripts. Subgroups of lncRNAs include competing endogenous RNAs, enhancer RNAs, and antisense RNAs, yet the majority of lncRNAs have not been categorized into functional subgroups. A further distinction is in regards to the transcriptional orientation of the lncRNA to its neighboring mRNA. Our work noted that IL-1β–regulated mRNA–lncRNA pairs are disproportionally divergently transcribed relative to IL-1β–regulated mRNA–mRNA pairs. These divergent mRNA–lncRNA pairs showed enrichment of RELA binding and H3K27ac marks in the intervening regions between them, suggesting that they share regulatory elements. Moreover, mRNAs near an IL-1β–regulated divergent lncRNA trended toward enhanced up-regulated response to IL-1β compared with those that were near a non-divergent lncRNA. These data are in line with evidence showing that promoters of divergent lncRNAs have higher activity than promoters of other classes of lncRNAs (42). However, in addition to sharing regulatory elements, we found that *lncRNA-CCL2* positively regulates its neighboring mRNA, *CCL2*. Other groups have also noted the high frequency of divergently transcribed neighboring mRNA–lncRNA pairs (18, 58). One of these groups successfully knocked down 16 divergent and antisense lncRNAs and found 10 of them to positively regulate the expression of their neighboring genes; meanwhile the other 6 divergent lncRNAs had no effect on their neighboring genes (18). It is intriguing that functional divergent lncRNAs, including *lncRNA-CCL2*, positively but never negatively regulated their neighboring genes. Thus, there may be something inherently unique to the function of divergent lncRNAs, and, in the future, there may be enough evidence for them to be considered as their own subclass of lncRNAs.

Teasing apart the mechanism of action of lncRNAs remains an arduous task due to the vast number of proteins that lncRNAs have been shown to interact with (30, 31). Adding to the complexity, some lncRNAs are found in both the nucleus and cytoplasm and have a distinct mechanism of action within each subcellular compartment (61). A systematic RNA fluorescence in situ hybridization screen of 61 lncRNAs revealed a wide range of distributions of lncRNAs throughout the cell. The majority of lncRNAs were found to be nuclear-enriched, but the amount present in the cytoplasmic fraction was highly variable (62). In the case of *lncRNA-CCL2*, it is detectable in both cellular compartments, with an enrichment in the cytoplasm, but our work has focused solely on the nuclear role of *lncRNA-CCL2* in regulating *CCL2* expression. We found that RNA-binding proteins that bind to nuclear *lncRNA-CCL2*, namely HNRNPU and IGF2BP2, can enhance or suppress *CCL2* transcript levels, respectively, without altering the abundance of *lncRNA-CCL2*. This implicates *lncRNA-CCL2* as a scaffold for RNA-binding proteins that may modulate *CCL2* expression in *cis*. An lncRNA expressed in adipocytes, *Linc-ADAL*, is also present in both the nuclear and cytoplasmic compartments, and, like *lncRNA-CCL2*, it has been shown to interact with HNRNPU and IGF2BP2. In the case of *Linc-ADAL*, it regulates levels of multiple mRNAs involved in adipocyte differentiation (49). Thus, it remains possible that *lncRNA-CCL2* may also act in *trans* to regulate other mRNAs via interaction with HNRNPU and IGF2BP2, and this should be investigated in future studies.

An additional layer of complexity to lncRNA function is discerning between the role of the lncRNA transcript itself vs. the contribution of transcription through the locus from which it is transcribed. The act of transcribing an lncRNA has previously been shown to mediate chromatin remodeling (63). In particular, halting lncRNA transcription through insertion of a polyA termination signal has been shown to influence neighboring gene expression via a decrease in enhancer marks (64). Given that

lncRNA-CCL2 is transcribed through a superenhancer, it is possible that its transcription could also have a functional consequence on enhancer activity. We attempted to use CRISPR/Cas9 to insert a polyA termination signal immediately after the first exon of *lncRNA-CCL2*. Despite the successful insertion of the polyA termination signal, we were unable to halt the transcription of *lncRNA-CCL2*. Perhaps the polyA signal was not strong enough to block the recruitment of abundant elongation factors and transcription machinery to the *CCL2* superenhancer (44). Another explanation could be that other TSSs are present within the *CCL2* superenhancer, which could give rise to an alternative *lncRNA-CCL2* transcript. It is therefore not possible, at the present time, to comment on the possible contribution of *lncRNA-CCL2* transcription to *CCL2* regulation. However, transcription alone cannot be solely responsible for its function, as targeted knock-down using siRNAs or GapmeRs directed to exon 2 was able to decrease *CCL2* mRNA levels without apparently impacting *lncRNA-CCL2* transcription.

Taken together, our studies have identified principals of dynamic lncRNA–mRNA networks in the setting of EC activation. We demonstrate that divergently transcribed lncRNAs located in the same TAD can positively regulate the expression of neighboring mRNAs during the inflammatory response. The applicability of lncRNAs for therapeutic intervention in vascular inflammatory diseases is exciting, but many questions remain. Their high cell type specificity makes them an attractive drug target due to fewer cell type off-target effects (59, 65). In our study, we found *lncRNA-CCL2* to be dysregulated in human atherosclerotic plaques. Therefore, exploring the therapeutic potential of *lncRNA-CCL2* may be of interest. A potential approach to target lncRNAs could be to use inhibitors to block the binding of lncRNAs to their interacting protein complexes. This approach has already been tested using "mixmer" oligomers, a mixture of LNA monomers combined with DNA monomers, in a spinal muscular atrophy model (66). Hence, using mixmers to block the interaction of *lncRNA-CCL2* with its interacting RNA-binding proteins, such as HNRNPU and IGF2BP2, could be of future interest to suppress vascular inflammation.

Methods

Cell Culture and Reagents. ECs utilized in this study included primary HUVEC (ScienCell 8000), immortalized human dermal microvascular ECs (HMEC1, ATCC CRL-3243), and immortalized HUVECs (EC-RF24, ABM T0003). HUVECs were cultured in Endothelial Cell Medium (ECM) with 5% FBS and Endothelial Cell Growth Supplement (ScienCell); meanwhile, HMEC1 and EC-RF24 were cultured in Endothelial Cell Media MV2 (PromoCell). Cells were treated with the following stimulants: IL-1β (10 ng/mL, Gibco), LPS (100 ng/mL, InvivoGen), TNFα (10 ng/mL, Gibco), VEGF (50 ng/mL, Gibco), TGFβ (10 ng/mL, Cell Signaling) for specified times. Cells were pretreated with the following inhibitors 1 h before IL-1β stimulation: TPCA-1 (IKK inhibitor, 3 μM, Sigma-Aldrich), C646 (p300 inhibitor, 10 μM, Sigma-Aldrich), JQ1 (BRD4 inhibitor, 500 nM, Sigma-Aldrich), and actinomycin D (transcriptional inhibitor, 5 μM, BioShop). All drugs were prepared as 1,000× stocks in dimethyl sulfoxide (DMSO). Human material analysis was performed as described in *SI Appendix*.

Cloning, Transfection, and Nucleoporation. Cells were transfected at 40% confluency with siRNAs and GapmeRs listed in *SI Appendix*, Table S1 using Lipofectamine RNAiMAX Reagent (1 μL/20 nM siRNA or GapmeR, Thermo Fisher Scientific) in Opti-MEM I Reduced Serum Media (100 μL, Thermo Fisher Scientific). Media was changed back to regular Endothelial Cell Media after 4 to 6 h, and cells were harvested after 48 h. For *lncRNA-CCL2* overexpression studies and in vitro transcription, *lncRNA-CCL2* was cloned into pCS2+ (Addgene #2295) (*SI Appendix*, Table S2). Alternatively, a *scramble* sequence of the same length as *lncRNA-CCL2* was cloned into pGEM-T Easy (Promega) for in vitro transcription (*SI Appendix*, Table S2). Overexpression experiments in HUVEC were performed using the P5 Primary Cell 4D-Nucleofector X Kit (Lonza) and the Amaxa 4D-Nucleofector System (Lonza) as per manufacturer's instructions for HUVEC using 1 μg of plasmid.

RNA Isolation, Reverse Transcription, and Quantitative PCR. RNA was isolated from cells using TRIzol Reagent (Thermo Fisher Scientific) as per the manufacturer's instruction. Nuclear fractionation was performed as described in *SI Appendix*. Reverse transcription was performed with between 500 ng to 1 μg RNA using the high-capacity cDNA reverse transcription kit (Applied Biosystems). The qRT-PCR was performed in triplicate using the LC480 SYBR Green I Master (Roche) and the Roche Lightcycler 480 (Roche). Data were analyzed using the delta–delta Ct method and were normalized to TATA-binding protein. Copy number quantification was performed using Roche Lightcycler 480 (Roche) using 10^7 to 10^3 copy numbers of qPCR products for the creation of a standard curve. Primers used are listed in *SI Appendix*, Tables S3 and S4.

Microarray Analysis. Expression changes of lncRNAs and mRNAs were assessed by the manufacturer using the Human LncRNA Expression Microarray V3.0 (Arraystar). The expression data were normalized using the Robust Multi-Array Average method. The lncRNAs and mRNAs were considered differentially expressed if they had a >2-fold change and were statistically significant (paired *t* test $P < 0.05$) for any of the time points of IL-1β treatment. Heatmaps were constructed using the "heatmap.2" function from the "gplots" Bioconductor package (67). Additionally, the "ggplot2," "sm," and "violinplot" Bioconductor packages were used for graph visualization. Neighboring transcript pairs were identified based on genomic distance (20 to 500 kbp) between them with the help of the "GenomicRanges" Bioconductor package (68). Spearman correlation coefficient (rho) was calculated using base R, and statistical significance between 2 rho values was determined using Fisher Z-transformation. ChIP followed by sequencing analysis was performed as described in *SI Appendix*.

RNA Pull-Down. RNA pull-down was performed as described elsewhere (69). To generate in vitro transcribed probes, *lncRNA-CCL2* was cloned downstream of the SP6 promoter in pCS2+ plasmid, and a *scramble* sequence of same length as *lncRNA-CCL2* was cloned downstream of the T7 promoter in pGEM-T Easy plasmid (*SI Appendix*, Table S2). In vitro transcription was performed using SP6 RNA Polymerase (P1085, Promega) and T7 RNA Polymerase (P2075, Promega) with the Biotin RNA Labeling Mix (Roche) using 1 μg of linearized plasmid. To pull down interacting partners, nuclear extracts from IL-1β–stimulated HMEC1 cells (5×10^6 cells per condition) were used. Precleared nuclear extracts were incubated with 1 μg of *lncRNA-CCL2* probe, *scramble* probe, or no probe. After pull-down, samples were either sent for mass spectrometry analysis (as described in *SI Appendix*) or run on Western blot (as described in *SI Appendix*). RNA immunoprecipitation was performed as described in *SI Appendix*.

Data Availability. Microarray data generated in this study have been deposited in the GEO database under the accession number GSE127990. Code used in the analysis can be accessed at https://github.com/nadiyakhyzha/lncRNA_mRNA_neighboring_analysis.

Statistical Analyses. Experiments were performed at least 3 times unless stated otherwise. Statistical analyses performed for each experiment are specified in the figure legends. $P < 0.05$ was considered to be statistically significant. Plotted data represent the mean ± SEM.

ACKNOWLEDGMENTS. We wish to thank Jonathan Krieger of SPARC BioCentre, The Hospital for Sick Children, Toronto, Canada, for assistance with mass spectrometry. This work was supported by Project Grants from the Canadian Institutes of Health Research (CIHR) (PJT 148487 [to J.E.F.] and 364832 [to J.E.F. and M.D.W.]). J.E.F. and M.D.W. were funded by CIHR Tier 2 Canada Research Chairs and Early Researcher Awards from the Ontario Ministry of Research and Innovation. J.E.F. was supported by a CIHR-funded Transnational Team Grant. Infrastructure in the J.E.F. laboratory was funded by the John R. Evans Leaders Opportunity Fund from the Canada Foundation for Innovation and the Ontario Research Fund. N.K. received a Canada Graduate Scholarship from the Natural Sciences and Engineering Research Council of Canada (NSERC). M.K. received an Undergraduate Student Research Award from NSERC. M.D.W. was supported by an NSERC grant (436194-2013). The BiKE project was financed by the Swedish Heart and Lung Foundation, Swedish Research Council, and Stockholm County Council. L. Maegdefessel is the recipient of fellowships from the Swedish Society for Medical Research and Heart and Lung Foundation, and is further supported by the European Research Council (Starting Grant NORVAS) and the German Center for Cardiovascular Research.

1. P. Libby, Inflammation in atherosclerosis. *Arterioscler. Thromb. Vasc. Biol.* **32**, 2045–2051 (2012).
2. S. Arslan *et al*., Cardiolinc™ network, Long non-coding RNAs in the atherosclerotic plaque. *Atherosclerosis* **266**, 176–181 (2017).
3. S. Cremer *et al*., Hematopoietic deficiency of the long non-coding RNA MALAT1 promotes atherosclerosis and plaque inflammation. *Circulation* **139**, 1320–1334 (2019).
4. A. Helgadottir *et al*., A common variant on chromosome 9p21 affects the risk of myocardial infarction. *Science* **316**, 1491–1493 (2007).
5. T. Sallam *et al*., Transcriptional regulation of macrophage cholesterol efflux and atherogenesis by a long noncoding RNA. *Nat. Med.* **24**, 304–312 (2018).
6. O. Jarinova *et al*., Functional analysis of the chromosome 9p21.3 coronary artery disease risk locus. *Arterioscler. Thromb. Vasc. Biol.* **29**, 1671–1677 (2009).
7. M. K. Atianand *et al*., A long noncoding RNA lincRNA-EPS acts as a transcriptional brake to restrain inflammation. *Cell* **165**, 1672–1685 (2016).
8. J. Chan *et al*., Cutting edge: A natural antisense transcript, AS-IL1α, controls inducible transcription of the proinflammatory cytokine IL-1α. *J. Immunol.* **195**, 1359–1363 (2015).
9. S. Carpenter *et al*., A long noncoding RNA mediates both activation and repression of immune response genes. *Science* **341**, 789–792 (2013).
10. X. Zhou *et al*., Long non-coding RNA ANRIL regulates inflammatory responses as a novel component of NF-κB pathway. *RNA Biol.* **13**, 98–108 (2016).
11. N. E. Ilott *et al*., Long non-coding RNAs and enhancer RNAs regulate the lipopolysaccharide-induced inflammatory response in human monocytes. *Nat. Commun.* **5**, 3979 (2014).
12. N. A. Rapicavoli *et al*., A mammalian pseudogene lncRNA at the interface of inflammation and anti-inflammatory therapeutics. *eLife* **2**, e00762 (2013).
13. C.-C. Hon *et al*., An atlas of human long non-coding RNAs with accurate 5′ ends. *Nature* **543**, 199–204 (2017).
14. M. N. Cabili *et al*., Integrative annotation of human large intergenic noncoding RNAs reveals global properties and specific subclasses. *Genes Dev.* **25**, 1915–1927 (2011).
15. S. Guil, M. Esteller, Cis-acting noncoding RNAs: Friends and foes. *Nat. Struct. Mol. Biol.* **19**, 1068–1075 (2012).
16. J. M. Engreitz *et al*., Local regulation of gene expression by lncRNA promoters, transcription and splicing. *Nature* **539**, 452–455 (2016).
17. J. Joung *et al*., Genome-scale activation screen identifies a lncRNA locus regulating a gene neighbourhood. *Nature* **548**, 343–346 (2017).
18. S. Luo *et al*., Divergent lncRNAs regulate gene expression and lineage differentiation in pluripotent cells. *Cell Stem Cell* **18**, 637–652 (2016).
19. S. Quinodoz, M. Guttman, Long noncoding RNAs: An emerging link between gene regulation and nuclear organization. *Trends Cell Biol.* **24**, 651–663 (2014).
20. J. T. Y. Kung, D. Colognori, J. T. Lee, Long noncoding RNAs: Past, present, and future. *Genetics* **193**, 651–669 (2013).
21. F. P. Marchese, I. Raimondi, M. Huarte, The multidimensional mechanisms of long noncoding RNA function. *Genome Biol.* **18**, 206 (2017).
22. S. Kaneko, J. Son, S. S. Shen, D. Reinberg, R. Bonasio, PRC2 binds active promoters and contacts nascent RNAs in embryonic stem cells. *Nat. Struct. Mol. Biol.* **20**, 1258–1264 (2013).
23. C. Cifuentes-Rojas, A. J. Hernandez, K. Sarma, J. T. Lee, Regulatory interactions between RNA and polycomb repressive complex 2. *Mol. Cell* **55**, 171–185 (2014).
24. A. A. Sigova *et al*., Transcription factor trapping by RNA in gene regulatory elements. *Science* **350**, 978–981 (2015).
25. X. Sun, M. S. S. Haider Ali, M. Moran, The role of interactions of long non-coding RNAs and heterogeneous nuclear ribonucleoproteins in regulating cellular functions. *Biochem. J.* **474**, 2925–2935 (2017).
26. P. A. Latos *et al*., Airn transcriptional overlap, but not its lncRNA products, induces imprinted Igf2r silencing. *Science* **338**, 1469–1472 (2012).
27. Y. Yin *et al*., Opposing roles for the lncRNA Haunt and its genomic locus in regulating HOXA gene activation during embryonic stem cell differentiation. *Cell Stem Cell* **16**, 504–516 (2015).
28. V. R. Paralkar *et al*., Unlinking an lncRNA from its associated *cis* element. *Mol. Cell* **62**, 104–110 (2016).
29. L. A. Goff *et al*., Spatiotemporal expression and transcriptional perturbations by long noncoding RNAs in the mouse brain. *Proc. Natl. Acad. Sci. U.S.A.* **112**, 6855–6862 (2015).
30. B. Signal, B. S. Gloss, M. E. Dinger, Computational approaches for functional prediction and characterisation of long noncoding RNAs. *Trends Genet.* **32**, 620–637 (2016).
31. F. Kopp, J. T. Mendell, Functional classification and experimental dissection of long noncoding RNAs. *Cell* **172**, 393–407 (2018).
32. J. R. Dixon, D. U. Gorkin, B. Ren, Chromatin domains: The unit of chromosome organization. *Mol. Cell* **62**, 668–680 (2016).
33. E. Melgarejo, M. A. Medina, F. Sánchez-Jiménez, J. L. Urdiales, Monocyte chemoattractant protein-1: A key mediator in inflammatory processes. *Int. J. Biochem. Cell Biol.* **41**, 998–1001 (2009).
34. S. Frank *et al*., yylncT defines a class of divergently transcribed lncRNAs and safeguards the T-mediated mesodermal commitment of human PSCs. *Cell Stem Cell* **24**, 318–327.e8 (2019).
35. C. F. Spurlock , 3rd *et al*., Expression and functions of long noncoding RNAs during human T helper cell differentiation. *Nat. Commun.* **6**, 6932 (2015).
36. M. S. Werner *et al*., Chromatin-enriched lncRNAs can act as cell-type specific activators of proximal gene transcription. *Nat. Struct. Mol. Biol.* **24**, 596–603 (2017).
37. T. Trimarchi *et al*., Genome-wide mapping and characterization of Notch-regulated long noncoding RNAs in acute leukemia. *Cell* **158**, 593–606 (2014).
38. J. R. Dixon *et al*., Topological domains in mammalian genomes identified by analysis of chromatin interactions. *Nature* **485**, 376–380 (2012).
39. E. P. Nora *et al*., Spatial partitioning of the regulatory landscape of the X-inactivation centre. *Nature* **485**, 381–385 (2012).
40. S. S. Rao *et al*., A 3D map of the human genome at kilobase resolution reveals principles of chromatin looping. *Cell* **159**, 1665–1680 (2014).
41. N. T. Hogan *et al*., Transcriptional networks specifying homeostatic and inflammatory programs of gene expression in human aortic endothelial cells. *eLife* **6**, e22536 (2017).
42. K. Mattioli *et al*., High-throughput functional analysis of lncRNA core promoters elucidates rules governing tissue specificity. *Genome Res.* **29**, 344–355 (2019).
43. R. J. Aiello *et al*., Monocyte chemoattractant protein-1 accelerates atherosclerosis in apolipoprotein E-deficient mice. *Arterioscler. Thromb. Vasc. Biol.* **19**, 1518–1525 (1999).
44. J. D. Brown *et al*., NF-κB directs dynamic super enhancer formation in inflammation and atherogenesis. *Mol. Cell* **56**, 219–231 (2014).
45. K. C. Wang *et al*., A long noncoding RNA maintains active chromatin to coordinate homeotic gene expression. *Nature* **472**, 120–124 (2011).
46. L. Wang *et al*., CPAT: Coding-Potential Assessment Tool using an alignment-free logistic regression model. *Nucleic Acids Res.* **41**, e74 (2013).
47. Y. Lu *et al*., The NF-κB-responsive long noncoding RNA FIRRE regulates posttranscriptional regulation of inflammatory gene expression through interacting with hnRNPU. *J. Immunol.* **199**, 3571–3582 (2017).
48. H. Nishitsuji *et al*., Long noncoding RNA #32 contributes to antiviral responses by controlling interferon-stimulated gene expression. *Proc. Natl. Acad. Sci. U.S.A.* **113**, 10388–10393 (2016).
49. X. Zhang *et al*., Interrogation of nonconserved human adipose lincRNAs identifies a regulatory role of *linc-ADAL* in adipocyte metabolism. *Sci. Transl. Med.* **10**, eaar5987 (2018).
50. M. Mineo *et al*., The long non-coding RNA HIF1A-AS2 facilitates the maintenance of mesenchymal glioblastoma stem-like cells in hypoxic niches. *Cell Rep.* **15**, 2500–2509 (2016).
51. Y. Hosono *et al*., Oncogenic role of THOR, a conserved cancer/testis long non-coding RNA. *Cell* **171**, 1559–1572.e20 (2017).
52. M. Yugami, Y. Kabe, Y. Yamaguchi, T. Wada, H. Handa, hnRNP-U enhances the expression of specific genes by stabilizing mRNA. *FEBS Lett.* **581**, 1–7 (2007).
53. N. Degrauwe, M. L. Suvà, M. Janiszewska, N. Riggi, I. Stamenkovic, IMPs: An RNA-binding protein family that provides a link between stem cell maintenance in normal development and cancer. *Genes Dev.* **30**, 2459–2474 (2016).
54. J. L. Bell *et al*., Insulin-like growth factor 2 mRNA-binding proteins (IGF2BPs): Post-transcriptional drivers of cancer progression? *Cell. Mol. Life Sci.* **70**, 2657–2675 (2013).
55. L. Perisic *et al*., Gene expression signatures, pathways and networks in carotid atherosclerosis. *J. Intern. Med.* **279**, 293–308 (2016).
56. A. V. Finn, M. Nakano, J. Narula, F. D. Kolodgie, R. Virmani, Concept of vulnerable/unstable plaque. *Arterioscler. Thromb. Vasc. Biol.* **30**, 1282–1292 (2010).
57. I. Tabas, G. García-Cardeña, G. K. Owens, Recent insights into the cellular biology of atherosclerosis. *J. Cell Biol.* **209**, 13–22 (2015).
58. A. A. Sigova *et al*., Divergent transcription of long noncoding RNA/mRNA gene pairs in embryonic stem cells. *Proc. Natl. Acad. Sci. U.S.A.* **110**, 2876–2881 (2013).
59. T. F. Brazão *et al*., Long noncoding RNAs in B-cell development and activation. *Blood* **128**, e10–e19 (2016).
60. A. Purmann *et al*., Genomic organization of transcriptomes in mammals: Coregulation and cofunctionality. *Genomics* **89**, 580–587 (2007).
61. L.-L. Chen, Linking long noncoding RNA localization and function. *Trends Biochem. Sci.* **41**, 761–772 (2016).
62. M. N. Cabili *et al*., Localization and abundance analysis of human lncRNAs at single-cell and single-molecule resolution. *Genome Biol.* **16**, 20 (2015).
63. K. Hirota *et al*., Stepwise chromatin remodelling by a cascade of transcription initiation of non-coding RNAs. *Nature* **456**, 130–134 (2008).
64. K. M. Anderson *et al*., Transcription of the non-coding RNA upperhand controls Hand2 expression and heart development. *Nature* **539**, 433–436 (2016).
65. C. Wahlestedt, Targeting long non-coding RNA to therapeutically upregulate gene expression. *Nat. Rev. Drug Discov.* **12**, 433–446 (2013).
66. C. J. Woo *et al*., Gene activation of SMN by selective disruption of lncRNA-mediated recruitment of PRC2 for the treatment of spinal muscular atrophy. *Proc. Natl. Acad. Sci. U.S.A.* **114**, E1509–E1518 (2017).
67. H. Wickham, H. Wickham, *ggplot2, Elegant Graphics for Data Analysis* (Springer), pp. 33–74 (2016).
68. M. Lawrence *et al*., Software for computing and annotating genomic ranges. *PLoS Comput. Biol.* **9**, e1003118 (2013).
69. O. Marín-Béjar, M. Huarte, RNA pulldown protocol for in vitro detection and identification of RNA-associated proteins. *Methods Mol. Biol.* **1206**, 87–95 (2015).